Received: 9 February 2024 | Revised: 25 July 2024 | Accepted: 2 August 2024

DOI: 10.1002/qj.4838

Quarterly Journal of the Royal Meteorological Society RMetS

RESEARCH ARTICLE

Precipitation enhancement over tropical land through the lens of the moisture–precipitation relationship

Luca Schmidt[1,2] | **Cathy Hohenegger**[1]

[1]Climate Physics Department, Max Planck Institute for Meteorology, Hamburg, Germany

[2]International Max Planck Research School on Earth System Modelling, Hamburg, Germany

Correspondence
Luca Schmidt, Climate Physics Department, Max Planck Institute for Meteorology, Hamburg, Germany.
Email: luca.schmidt@mpimet.mpg.de

Funding information
Max Planck Society

Abstract

Tropical precipitation P has been found to be related to column relative humidity r by a simple relationship known as the moisture–precipitation relationship $P(r)$. Based on one decade of daily ERA5 reanalysis data, we test whether $P(r)$ is able to reproduce the tropical land–ocean precipitation contrast measured by χ, the ratio between mean precipitation over land and ocean. We find that $P(r)$ captures the mean seasonal cycle of χ as long as we account for the fact that $P(r)$ is distinct over land and ocean, and that it varies seasonally. Typical values of χ above 0.86 imply that precipitation is enhanced over land, relative to the ocean. We therefore investigate next whether this enhancement is due to the differences in $P(r)$ and/or in the humidity distribution between land and ocean. We show that, rather than enhancing precipitation, the presence of land modifies $P(r)$ in such a way that precipitation over land is disfavored compared to over ocean. Precipitation enhancement over land is instead explained by the modified terrestrial humidity distribution that features a more pronounced tail towards high r values compared to the one over ocean. All results rest on an accurate construction of $P(r)$ from the underlying data. Simple fit models such as an exponential function that were proposed by previous studies are unable to capture the seasonal cycle of χ and fail to explain land–ocean differences in precipitation.

KEYWORDS

ERA5, land–atmosphere interactions, relative humidity, tropical precipitation

1 | INTRODUCTION

Tropical precipitation is related to atmospheric humidity through a statistical, roughly exponential relationship, known as the moisture–precipitation relationship. Using satellite observations, Bretherton *et al.* (2004) showed that this moisture–precipitation relationship holds over all tropical oceans. A similar, albeit not identical, moisture–precipitation relationship was found over tropical land (Ahmed & Schumacher, 2017; Schiro *et al.*, 2016). In this work, we investigate what the moisture–precipitation relationship can teach us about the controls on the land–ocean contrast of tropical mean precipitation.

The land–ocean contrast of tropical mean precipitation can be quantified by the precipitation ratio χ, which denotes the ratio of spatiotemporal mean precipitation over tropical land and ocean, with the Tropics being defined as the region between 30°S and 30°N. Hohenegger and Stevens (2022) found climatological values of χ between 0.90 and 1.04 in observations. These values close to 1 indicate similar mean precipitation rates over tropical land and tropical ocean, and therefore suggest the absence of any climatological land–ocean difference in area-averaged precipitation amounts. However, Hohenegger and Stevens (2022) show that this interpretation is erroneous: Most tropical precipitation occurs in a narrow longitudinal band, also known as the "tropical rain belt", which migrates seasonally between about 15°S and 15°N. In this latitudinal range, the land fraction is smaller than the land fraction of the full Tropics (30°S to 30°N). If mean precipitation rates within the tropical rain belt were to be identical over land and ocean, and if no precipitation were to occur outside the rain belt—a reasonably good approximation according to Hohenegger and Stevens (2022, fig. 1)—then the smaller land fraction seen by the rain belt compared with the whole Tropics would lead to a precipitation ratio of $\chi \approx 0.86$ rather than 1. The fact that χ values obtained from observations lie above 0.86 indicates an enhancement of precipitation over tropical land. The theoretical value of $\chi = 0.86$ serves as a threshold for diagnosing this enhancement. Whereas Hohenegger and Stevens (2022) explained the observed precipitation enhancement over tropical land in terms of modifications of the rain belt's characteristics such as width, location, and intensity, by the land surface, the present work examines this precipitation enhancement through the lens of the moisture–precipitation relationship.

The moisture–precipitation relationship $P(r)$, which links mean precipitation rate P to column relative humidity r, was formally introduced by Bretherton *et al.* (2004), but several previous works, such as the early study by Austin (1948) or the later studies by Raymond and Torres (1998) and Tompkins (2001), already described a strong correlation between precipitation and ambient humidity, in particular humidity of the lower free troposphere. Various explanations for this strong correlation were proposed in the literature, including the impact of lateral entrainment of dry/moist air on plume buoyancy (e.g., Derbyshire *et al.*, 2004; Holloway & Neelin, 2009; Tompkins, 2001), convective downdrafts that inject moist air into the boundary layer, thereby changing the boundary-layer stability (e.g., Muller *et al.*, 2009; Tompkins, 2001), or tropical convection as an instance of self-organized criticality in the context of continuous phase transitions (Peters & Neelin, 2006).

Owing to its simplicity and apparent generality, analytical formulations of $P(r)$ have been used to parametrize precipitation in conceptual models. We employed $P(r)$ as a parametrization in a previous study aiming at understanding the controls on χ using a simple box model based on water balance equations (Schmidt & Hohenegger, 2023). Consistent with Hohenegger and Stevens (2022), even though methodologically independent, we found that precipitation enhancement over tropical land, as observed in the real world, requires the land surface to influence the way it rains. In the framework of the box model, in which humidity over land and ocean are each represented by a single mean value, this implies that the moisture–precipitation relationship must be distinct over land and ocean such that it rains more over land for a given value of r. Ahmed and Schumacher (2017) analyzed differences in $P(r)$ between various tropical land and ocean regions and indeed found systematic differences between the two surface types. Over land, $P(r)$ typically picks up at an earlier threshold value of r but then flattens more towards high r. Thus, the $P(r)$ curve over land does not generally lie above the one over ocean, but only in some range of r. Apart from the moisture–precipitation relationship, also the humidity distributions over land and ocean can be expected to be distinct but such differences were not investigated by Ahmed and Schumacher (2017). It is therefore not clear whether differences in $P(r)$ or in the humidity distributions explain precipitation enhancement over land, and which range of r is key to the enhancement.

The aim of this study is to investigate which features of $P(r)$ or differences in the terrestrial and oceanic humidity distributions explain the enhancement of precipitation over tropical land. To this end, we first describe in Section 2 the data and methodology employed. In Section 3, we evaluate on which spatial and temporal scale we need to sample the variability of $P(r)$ in order to correctly capture the mean behavior of χ over time. In Section 4, we use the moisture–precipitation relationships obtained and perform sensitivity experiments that disentangle the role of distinct $P(r)$ relationships and distinct humidity distributions over land and ocean in creating precipitation enhancement over tropical land. Finally, we reflect on the dependence of our results on the fit model employed in Section 5, and conclude with a general summary of our findings in Section 6.

2 | DATA AND METHODS

In this work, we assess whether the moisture–precipitation relationship $P(r)$, defined as the relationship between the daily mean precipitation rate P (mm·day^{-1})

and daily mean column relative humidity r, can explain the precipitation enhancement over tropical land, which is indicated by values of the tropical precipitation ratio higher than 0.86 (Hohenegger & Stevens, 2022). The tropical precipitation ratio is computed as

$$\chi(t) = \frac{\overline{P_\ell}(t)}{\overline{P_o}(t)}, \quad (1)$$

where $\overline{P_\ell}(t)$ represents the daily mean precipitation averaged over tropical land, and $\overline{P_o}(t)$ is the daily mean precipitation averaged over tropical ocean. The units of $\overline{P_\ell}$ and $\overline{P_o}$ are millimeters per day, and t denotes time in days.

2.1 | Data selection and variables

The study is based on 10 years of European Centre of Medium-range Weather Forecasts Reanalysis v5 (ERA5) data with a grid spacing of 30 km (Hersbach *et al.*, 2018a, 2018b). We consider the Tropics as 30°S to 30°N, and we select the time period from 1981 to 1990 for two reasons. First, the ERA5 precipitation ratio χ shows no significant trend related to, for instance, global warming, in this period. Second, a positive ERA5 precipitation bias over tropical oceans emerges around the year 1990 (Hersbach *et al.*, 2020), which leads to a negative bias in χ in subsequent decades. In the 1980s, ERA5 precipitation already benefits from the assimilation of satellite data, and the mean seasonal cycle of χ is similar to the one derived directly from Tropical Rainfall Measuring Mission satellite observations—compare Figure 1 with Hohenegger and Stevens (2022, fig. 6b).

To evaluate Equation (1) and to derive the $P(r)$ relationship, we use fields of daily mean precipitation P, as well as daily mean column relative humidity r. Column relative humidity is defined as the ratio of column-integrated specific humidity and column-integrated saturation specific humidity. To obtain daily r values, we first compute column relative humidity from hourly fields of temperature T (K), specific humidity q_v (kg·kg^{-1}), and pressure p (Pa) and then perform the daily averaging. The saturation vapor pressure, which is needed for the computation of saturation specific humidity, is calculated according to Murphy and Koop (2005, eq. 10). Note that the ERA5 data contain non-zero entries for atmospheric variables of subsurface grid cells that need to be masked before computing vertical integrals over the atmospheric column.

2.2 | Reconstruction of $\chi(t)$ from $P(r)$

To understand the controls on the tropical precipitation ratio through the lens of the moisture–precipitation relationship, we first have to find out what we need to know about $P(r)$ to reconstruct the ERA5 $\chi(t)$ from it. This reconstruction happens in two steps. First, we derive the functional relationship $P(r)$ as an empirical fit to the P and r data. To this end, we take pairs of (P, r) and sort them by ascending r. Next, we divide the r-space, ranging from 0 to 1, into bins of length 0.01, assign the pairs of (P, r) to their respective bin and average the precipitation within each bin. The empirical fit is then the piecewise linear function connecting the bin-mean precipitation values along r. In the second step, we reconstruct daily precipitation fields by applying the $P(r)$ fit obtained to the daily r values from ERA5. The reconstructed precipitation ratio $\chi_{rec}(t)$ can then be computed from the reconstructed precipitation fields using Equation (1).

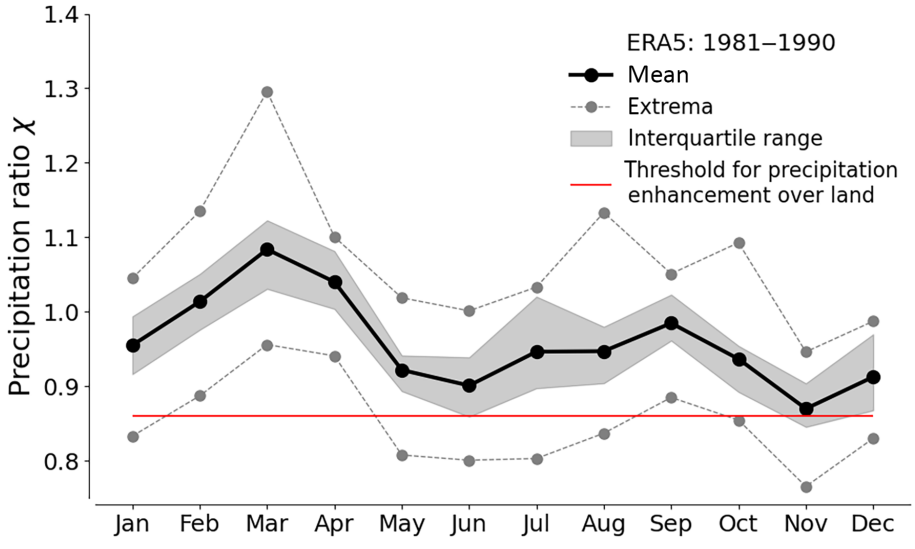

FIGURE 1 Mean seasonal cycle (solid black line) of the precipitation ratio from European Centre of Medium-range Weather Forecasts Reanalysis v5 (ERA5) data from 1981 to 1990. The interannual variability is shown by the interquartile range of values from individual years (shaded area) and by the extreme values for each month (dashed lines). The red line shows the threshold for precipitation enhancement over land as identified by Hohenegger and Stevens (2022). [Colour figure can be viewed at wileyonlinelibrary.com]

To complete the first step, we need to make two choices. First, we need to decide on the spatial and temporal resolutions of the P and r data. Second, we need to decide over which temporal and spatial scales we sample P and r when deriving the empirical fit. In other words, how many empirical fits do we need to adequately account for the variability of the moisture–precipitation relationship in space and time? Regarding the first choice, we decided to use daily (rather than, for example, monthly) P and r data as well as the native grid resolution. This choice was based on two considerations. First, the physical mechanisms proposed as explanations for the tight relationship between P and r, such as entrainment of convective plumes, act locally and on short temporal scales. Second, nonlinear relationships such as $P(r)$ are not scale invariant, meaning that averaging over r and P values in space or time not only reduces the sampled range of r and P values, it also results in a loss of information about the shape of the relationship. The second choice, namely the spatial and temporal scale for sampling P and r, is investigated in the next section, since it will give us a first answer as to how important land–ocean differences are for reconstructing $\chi(t)$ and, hence, for explaining precipitation enhancement over tropical land.

3 | WHAT DO WE NEED TO KNOW ABOUT $P(r)$ TO CORRECTLY RECONSTRUCT $\chi(t)$?

Apart from the dependence of the retrieved $P(r)$ relationship on the resolution of the underlying data discussed in Section 2.2, the physical relationship itself may be subject to variability in space and time. To assess this, we compute reconstructions $\chi_{\mathrm{rec}}(t)$ from $P(r)$ fit functions that reflect increasingly detailed spatial and temporal knowledge about $P(r)$. The metric for deciding whether the knowledge of $P(r)$ is detailed enough is the comparison of the mean seasonal cycle and year-to-year variability of the reconstructed $\chi_{\mathrm{rec}}(t)$ with the benchmark $\chi_{\mathrm{bm}}(t)$, where $\chi_{\mathrm{bm}}(t)$ is computed directly from the 10-year ERA5 daily precipitation fields using Equation (1). Figure 1 shows the mean seasonal cycle of $\chi_{\mathrm{bm}}(t)$ with a solid black line. The year-to-year variability is represented in terms of the interquartile range (gray shading) and 10-year extrema of monthly mean values (dashed lines). Throughout this work, we use the mean and interquartile range as the benchmark against which we test different reconstructions $\chi_{\mathrm{rec}}(t)$. The expectation is that these statistical characteristics of $\chi_{\mathrm{bm}}(t)$ will only be captured correctly by $\chi_{\mathrm{rec}}(t)$ if the knowledge of the underlying $P(r)$ relationship(s) is sufficiently detailed.

3.1 | The surface type, being land or ocean, modifies the shape of $P(r)$

As a first step, we compute $\chi_{\mathrm{rec}}(t)$ based on one $P(r)$ relationship derived from all pairs (P, r), which assumes that the same $P(r)$ relationship holds across the full Tropics and does not vary with time. This full tropical fit is shown in Figure 2a by the gray line. Owing to the high nonlinearity of $P(r)$, we use a logarithmic scale for the vertical axis. Further, for better visibility of the relevant ranges of r, we do not display values below $r = 0.3$ as they only contribute insignificantly small amounts of precipitation.

Figure 3a shows the corresponding reconstruction of $\chi(t)$ from the full tropical fit in blue as well as the benchmark in black. The reconstruction from the full tropical fit grossly overestimates $\chi_{\mathrm{bm}}(t)$, especially in boreal summer. This overestimation is both due to an overestimation of $\overline{P_\ell}(t)$ by up to 24.58% and an underestimation of $\overline{P_{\mathrm{o}}}(t)$ by up to 1.23%. That the reconstruction bias is dominated by a misrepresentation of land precipitation is a first indication for a systematic difference between the two surface types. The full tropical fit not only overestimates the overall magnitude of $\chi_{\mathrm{bm}}(t)$, it also misrepresents the seasonal variations.

Both reconstruction biases resulting from the full tropical fit can also be seen in Figure 3b, which shows a scatter plot of the monthly mean values of $\chi_{\mathrm{rec}}(t)$ from all individual years against the respective benchmark values. The identity line is plotted as a gray dashed line for visual guidance. Most scatter points lie below the identity line, owing to the overestimation of $\chi_{\mathrm{bm}}(t)$, and the spread of the scatter cloud is rather large due to the mismatch between the seasonal cycles of $\chi_{\mathrm{rec}}(t)$ and $\chi_{\mathrm{bm}}(t)$. This mismatch is quantified by the Pearson correlation coefficient c, for which we obtain the relatively low value of $c = 0.68$.

In a second step, we test whether accounting for a potential modification of $P(r)$ by the underlying surface type improves the reconstruction. To this end, we compute separate fits $P_\ell(r)$ and $P_{\mathrm{o}}(r)$ to data from land grid cells (P_ℓ, r_ℓ) and ocean grid cells $(P_{\mathrm{o}}, r_{\mathrm{o}})$ respectively. The two fits are displayed in Figure 2a, where the orange line represents $P_\ell(r)$ and the blue line represents $P_{\mathrm{o}}(r)$. Not surprisingly, the ocean fit is similar to the full tropical fit due to the larger areal extent of the ocean compared with land. There exist notable differences between $P_\ell(r)$ and $P_{\mathrm{o}}(r)$, which can be broadly described in terms of three regimes along r: For $r \lessapprox 0.6$, the mean precipitation is higher over ocean than over land; for $0.6 \lessapprox r \lessapprox 0.78$, the land fit exhibits a "bump," such that the mean precipitation is higher over land than over ocean; and for values of $r \gtrapprox 0.78$, the mean precipitation is again higher over ocean. These regimes of qualitatively different behavior over land and ocean

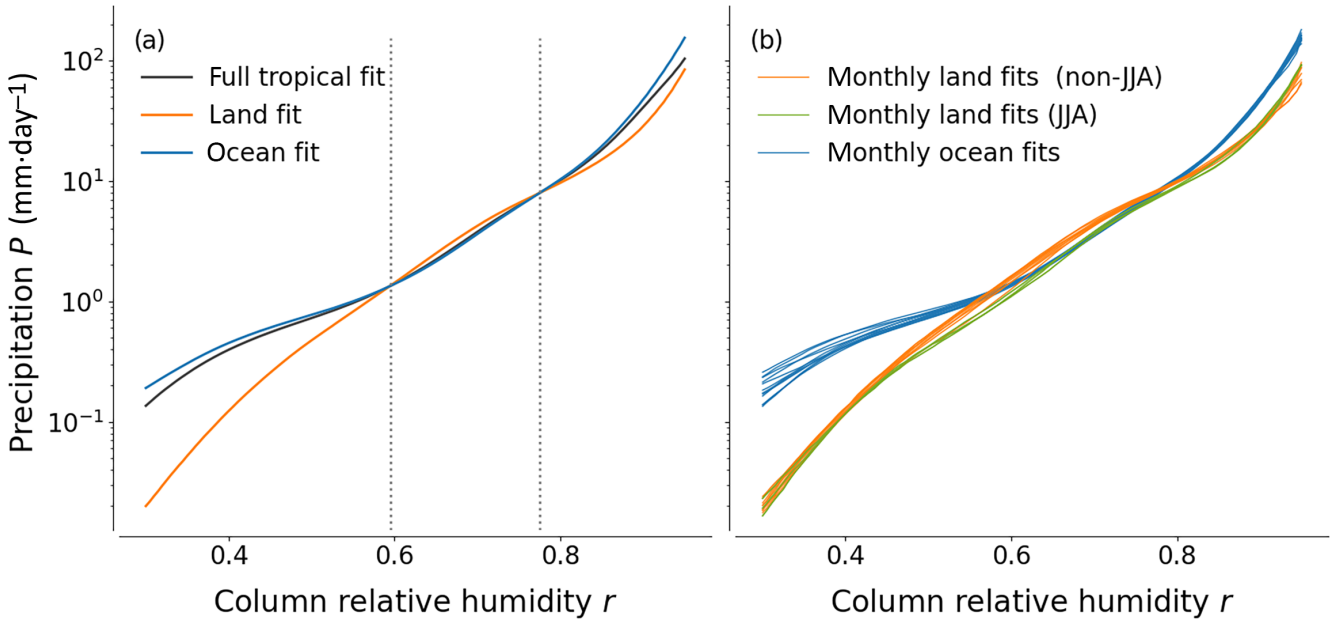

FIGURE 2 Empirical fit functions of the moisture–precipitation relationship in log-space obtained from different subsets of the underlying daily (P, r) data. The gray line in (a) shows the full tropical fit based on all tropical grid points, whereas the orange/green and blue lines in both (a) and (b) show the land and ocean fits, computed from tropical land and ocean grid points, respectively. (a) Fits based on the complete 10-year data set; (b) 12 fits derived for the individual months. Vertical dashed lines in (a) mark the approximate intersection points of the land and ocean relationships and divide the humidity space into three different r regimes. The land fits for June, July, and August (JJA) in (b) are colored green to indicate that they do not exhibit the "bump", relative to the ocean lines, which characterizes the middle r regime. [Colour figure can be viewed at wileyonlinelibrary.com]

hint at a complex interaction between surface type and $P(r)$ that may not necessarily lead to an enhancement of precipitation over land and which we disentangle further in Section 4. It needs to be noted, however, that observational studies of land–ocean differences in $P(r)$ do not report the low-r regime in which mean ocean precipitation rates exceed land precipitation rates (e.g., Ahmed & Schumacher, 2017, fig. 1). Rather, the existence of this regime might be related to difficulties of the convection scheme underlying the ERA5 data to produce realistic precipitation rates in dry environments (Derbyshire *et al.*, 2004). We will discuss further the potential influences of ERA5 biases on our results in Section 6.

Figure 3c,d displays how $\chi_{\mathrm{rec}}(t)$ is improved by using the surface-type-specific functions $P_\ell(r)$ and $P_{\mathrm{o}}(r)$ for reconstructing precipitation over land and ocean, respectively. Accounting for the surface type corrects the general overestimation such that, this time, $\chi_{\mathrm{rec}}(t)$ and $\chi_{\mathrm{bm}}(t)$ have the same 10-year mean value of 0.96 and the scatter points in Figure 3d lie more symmetrically around the identity line. However, seasonal reconstruction biases persist, with an overestimation from May to August and an underestimation otherwise. Owing to these seasonal biases, the correlation is only slightly improved, with a correlation coefficient of $c = 0.72$.

3.2 | $P(r)$ exhibits significant seasonal variations

The seasonally varying biases in the reconstruction that remain after taking into account the land–ocean contrast of the moisture–precipitation relationship suggest a distinct seasonal cycle of $P(r)$ over one or both of the two surface types. In a third step, we therefore derive 12 monthly relationships $P_{\ell,m}(r)$ and $P_{\mathrm{o},m}(r)$, for each surface type, with m specifying the month. These monthly mean relationships, again computed from the 10 years of daily data but conditioned on month m, are shown in Figure 2b as orange/green lines for the land and blue lines for the ocean. The three green lines correspond to June, July, and August (JJA), and are highlighted due to their qualitatively distinct behavior relative to the corresponding ocean curve. Generally, the variability is stronger over land than over ocean, except for low r values. This variability leads to qualitative changes of the land–ocean contrast of $P(r)$ over the course of the year, in that the "bump", in $P_\ell(r)$, constituting the middle r regime where it rains more over land than over ocean, disappears during JJA. In JJA, there is consequently no range of r in which $P_\ell(r)$ lies above $P_{\mathrm{o}}(r)$, which means that our initial hypothesis from our box model can already be refuted for these months.

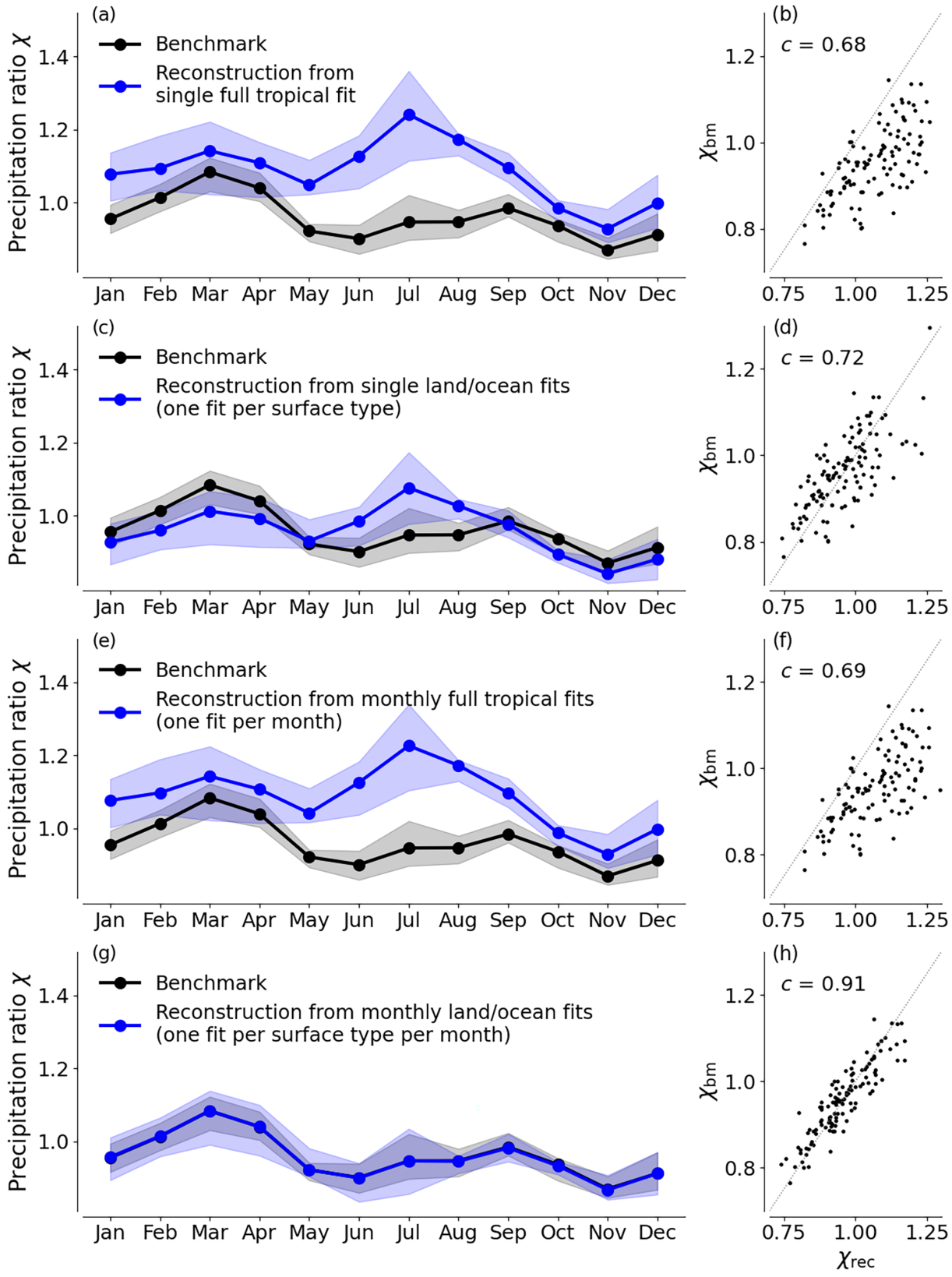

FIGURE 3 Comparison of benchmark $\chi_{bm}(t)$ with different reconstructions $\chi_{rec}(t)$ based on moisture–precipitation relationships that were fitted to different subsets of the daily data as shown in Figure 2 (monthly full tropical fits not shown). (a, c, e, g) The 10-year mean seasonal cycle (solid lines) and interquartile ranges of monthly mean values from individual years (shading). (b, d, f, h) Monthly mean values of individual years (1981–1990) from benchmark and reconstruction plotted against each other. The gray dashed line shows the identity line, $\chi_{bm} = \chi_{rec}$, and c denotes the Pearson correlation coefficient. [Colour figure can be viewed at wileyonlinelibrary.com]

As we account for the seasonal cycle of the moisture–precipitation relationship in the reconstruction of $\chi(t)$ by using the monthly fit functions $P_{o,m}(r)$ and $P_{\ell,m}(r)$, the seasonal biases disappear, as shown in Figure 3g,h. The mean curves of $\chi_{rec}(t)$ and $\chi_{bm}(t)$ lie now nearly perfectly on top of each other, and the correlation coefficient increases substantially to a value of $c = 0.91$. Note that the seasonal cycle over land is more relevant for a correct reconstruction of $\chi_{bm}(t)$ than the one over ocean, but neglecting the seasonality of $P_o(r)$ nevertheless introduces reconstruction biases of up to 3.7%. Even though the interquartile range in Figure 3g is still overestimated in most months, we deem this reconstruction from monthly land/ocean fits to be accurate enough to neglect higher order spatial and temporal variations of $P(r)$.

One may ask whether accounting for monthly variations of $P(r)$ alone (i.e., using monthly full tropical fit functions) would lead to a sufficiently accurate reconstruction, rendering the distinction between land and ocean obsolete. To test this, we compute the reconstruction from a month-dependent full tropical fit, shown in Figure 3e, and find a very similar picture to the reconstruction based on the full tropical fit without monthly distinctions (Figure 3a), with only a marginal improvement of the correlation shown in Figure 3f. This similarity is explained by the dominance of ocean grid points in setting the full tropical fit. Since the oceanic moisture–precipitation relationship shows only a weak seasonality, this feature is imposed on the full tropical relationship.

In conclusion, we find that the surface type is a meaningful criterion for the spatial variability of the moisture–precipitation relationship but that, on top of this, month-to-month variability needs to be taken into account in order to be able to adequately reconstruct characteristic features of the time evolution of the tropical precipitation ratio. Building on these insights, we can now investigate whether, at least in months other than JJA, the land–ocean differences in the moisture–precipitation relationship are responsible for precipitation enhancement over tropical land, and what role the underlying humidity distribution plays.

4 | PRECIPITATION ENHANCEMENT OVER TROPICAL LAND

Following the theoretical results found by Hohenegger and Stevens (2022), we diagnose precipitation enhancement over tropical land whenever $\chi > 0.86$. Figure 1 shows that the mean value of χ_{bm} lies above this threshold in all months, consistent with observations (see Hohenegger and Stevens (2022, fig. 5a)), even though individual years sometimes fall below it.

4.1 | Is the land–ocean contrast of $P(r)$ responsible for precipitation enhancement over land?

One possible explanation for the precipitation enhancement over tropical land, inspired by a previous box model study based on water balance equations (Schmidt & Hohenegger, 2023), is that the presence of land modifies the moisture–precipitation relationship such that P is larger over land than over ocean for a given value of r.

We test this explanation by conducting a sensitivity experiment. We assume that the land does not modify the moisture–precipitation relationship and reconstruct both land and ocean precipitation using the oceanic relationship $P_{o,m}(r)$. If the modification of $P(r)$ by the land surface is the key mechanism responsible for precipitation enhancement over tropical land, then we expect to see an underestimation of $\chi_{bm}(t)$ by $\chi_{rec}(t)$ due to an underestimation of mean land precipitation $\overline{P_\ell}$, and χ_{rec} values should typically lie below 0.86.

Given that $P_{o,m}(r)$ is very close to the tropical fit, we can already guess that this will not be the case. And indeed, Figure 4a reveals an overestimation in all months. Hence, all land–ocean differences in the moisture–precipitation relationships combined act to disfavor land precipitation and are generally not the reason why we observe precipitation enhancement over tropical land. Note that this result is independent of the choice of applying $P_{o,m}(r)$ over both land and ocean, rather than $P_{\ell,m}(r)$.

What is not yet fully clear is whether the "bump", as the only r range in which precipitation rates over land are higher than over ocean, is needed for χ to lie above the threshold of 0.86. To investigate the role of the "bump", we perform a similar experiment as before but this time we only set $P_{\ell,m}(r) = P_{o,m}(r)$ within the range of r that constitutes the "bump." The corresponding reconstruction is shown in Figure 4b. As expected, χ_{rec} is reduced compared with χ_{bm} in all months in which a "bump" was present. However, except for November, where precipitation enhancement over land was very weak to begin with, the blue reconstruction curve still lies above the threshold of $\chi = 0.86$, implying that the "bump", is not necessary for precipitation enhancement over land either.

4.2 | Precipitation enhancement over land due to different humidity distributions

As the distinct moisture–precipitation relationships over land and ocean are not the reason for precipitation

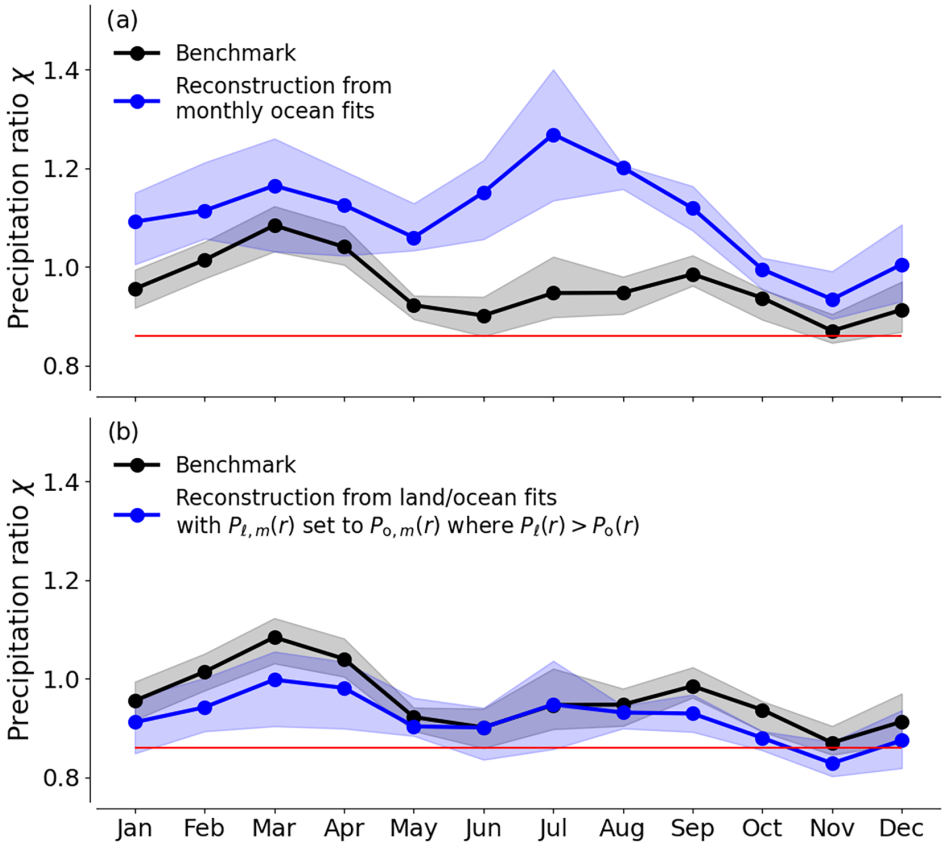

FIGURE 4 Comparison of the benchmark precipitation ratio with reconstructions from sensitivity experiments. (a) Reconstructed precipitation over both land and ocean was computed from the oceanic relationship $P_{o,m}(r)$. (b) Reconstructed ocean precipitation was computed from $P_{o,m}(r)$ and reconstructed land precipitation was computed from a modified land relationship which was set to $P_{o,m}(r)$ in the range where $P_{\ell,m}(r) > P_{o,m}(r)$, effectively removing the "bump." The threshold for precipitation enhancement over land is shown in red. [Colour figure can be viewed at wileyonlinelibrary.com]

enhancement over land, the enhancement has to be due to distinct humidity distributions. This prompts the question of how the humidity distributions over land and ocean differ in the first place. In addition, we want to know which ranges of r are particularly relevant for explaining precipitation enhancement over land. The relevance of different ranges of r cannot be discerned from the humidity distributions alone but only from the combined effect of the distinct humidity distributions, which set how numerous grid cells with a given value of r are, and the effect of the distinct moisture–precipitation relationships, which set how much precipitation is expected from that given value of r.

Figure 5 shows the moisture–precipitation relationships (top row) and probability density functions of column relative humidity $f(r)$ (second row) for three exemplary months. For each month, the underlying data are combined from all 10 years. Land and ocean quantities are shown as orange and blue lines respectively. In all months, the humidity distribution over land exhibits a much stronger bimodality than over ocean, with a first peak around $r = 0.2$ and a second, stronger, peak around $r = 0.75$. Over ocean, some bimodality can be discerned as well, but peak magnitudes are more similar and the first peak occurs at a higher r value around 0.45 whereas the second peak appears close to the second land peak at around $r = 0.75$.

How these land–ocean differences in the humidity distribution matter, for explaining the enhancement of precipitation over land depends on their combination with differences in the moisture–precipitation relationship. We selected March, July, and November as examples because these months represent three qualitatively distinct combinations of features of $P(r)$ and $f(r)$: March and July have in common that the land humidity distribution has a pronounced tail towards high r values, but the two months differ in that March exhibits the "bump" in the moisture–precipitation relationship over land whereas July does not. November exhibits the "bump" as well but is different from March in that its humidity distribution has a more pronounced high-r tail over ocean rather than over land. In the following, we analyze how these features interact to enhance precipitation over land and attribute the enhancement to specific ranges of r.

To this end, we recast the formulation of the 10-year monthly mean precipitation ratio $\chi_{\text{mean},m}$ in the framework of the moisture–precipitation relationships and humidity distributions:

$$\chi_{\text{mean},m} = \frac{\int_0^1 P_{\ell,m}(r) f_{\ell,m}(r)\, dr}{\int_0^1 P_{o,m}(r) f_{o,m}(r)\, dr}, \tag{2}$$

where $f_{\ell,m}(r)$ and $f_{o,m}(r)$ are the monthly land and ocean humidity distributions, respectively. To evaluate the

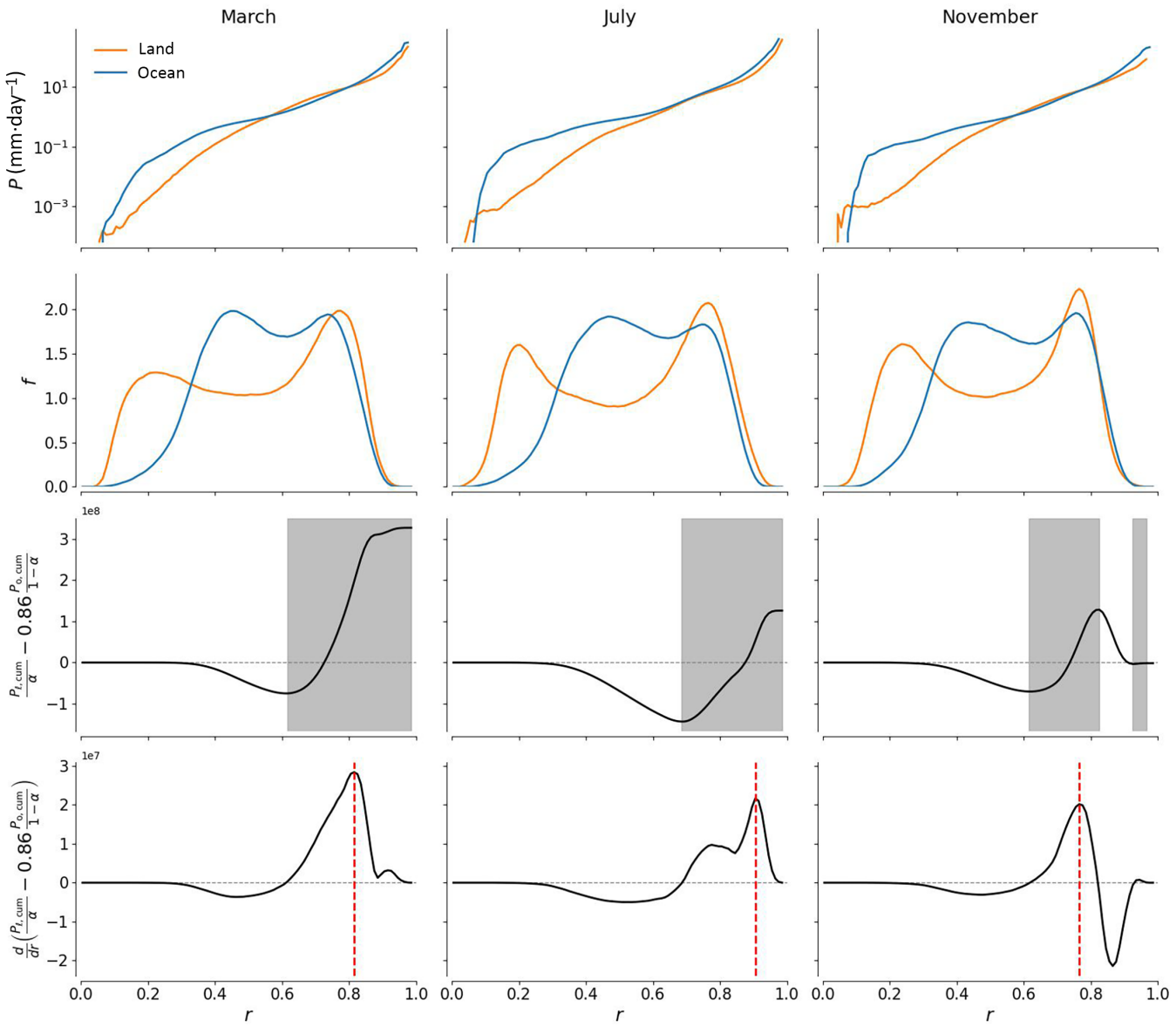

FIGURE 5 Land and ocean moisture–precipitation relationships (top row) and probability density functions of column relative humidity (second row) for three exemplary months. The third row shows the curves of the left-hand side of Equation (6) in black. Ranges of r that contribute to precipitation enhancement over land are those in which the black curves exhibit a positive slope and are marked with gray shading. The bottom row shows the rate of change of the left-hand side of Equation (6) along r, with the red dashed line indicating the location of maximum increase. [Colour figure can be viewed at wileyonlinelibrary.com]

integrals in Equation (2), we express the humidity distributions in terms of area fractions of grid cells with a given value of r:

$$f_{\ell,m}(r) = \frac{A_{\ell,m}(r)}{\int_0^1 A_{\ell,m}(r)\,dr} = \frac{A_{\ell,m}(r)}{\alpha A_{\mathrm{tr},m}}, \tag{3}$$

$$f_{\mathrm{o},m}(r) = \frac{A_{\mathrm{o},m}(r)}{\int_0^1 A_{\mathrm{o},m}(r)\,dr} = \frac{A_{\mathrm{o},m}(r)}{(1-\alpha) A_{\mathrm{tr},m}}, \tag{4}$$

where $A_{\ell/\mathrm{o},m}(r)$ denotes the 10-year total area of grid cells with the given value of r over either land or ocean, $\alpha \approx 0.26$ denotes the tropical land fraction, and $A_{\mathrm{tr},m}$ is the total area of the Tropics between 30°S and 30°N multiplied by the number of days in month m from all 10 years. Even though mathematically not identical, $\chi_{\mathrm{mean},m}$ is practically equivalent to the mean seasonal cycle of $\chi(t)$ computed in Section 3 (solid lines in Figure 3g). Replacing the humidity distributions in Equation (2) by the right-hand side expressions of Equations (3) and (4), we can now formulate the condition for precipitation enhancement over tropical land as

$$\chi_{\mathrm{mean},m} = \frac{\frac{1}{\alpha}\int_0^1 P_{\ell,m}(r) A_{\ell,m}(r)\,dr}{\frac{1}{1-\alpha}\int_0^1 P_{\mathrm{o},m}(r) A_{\mathrm{o},m}(r)\,dr} > 0.86. \tag{5}$$

Since we want to assess which ranges of r contribute to precipitation enhancement over land, we make use of the fact that the integrals in Equation (5) are equivalent to the cumulative 10-year total rainfall over land and ocean, $P_{\ell,\mathrm{cum}}(r_\mathrm{s}, r_\mathrm{e})$ and $P_{\mathrm{o,cum}}(r_\mathrm{s}, r_\mathrm{e})$ respectively, where the accumulation is performed along r, starting from $r_\mathrm{s} = 0$ and ending at $r_\mathrm{e} = 1$. With $r_\mathrm{s} = 0$ fixed and r_e as the variable end point of the accumulation, we rewrite Equation (5) as

$$\frac{P_{\ell,\mathrm{cum}}(r_\mathrm{e})}{\alpha} - 0.86\frac{P_{\mathrm{o,cum}}(r_\mathrm{e})}{1-\alpha} > 0 \tag{6}$$

and identify ranges of r that contribute to precipitation enhancement over land as those in which the term on the left-hand side (LHS) of Equation (6) increases.

We evaluate the LHS of Equation (6) and its derivative with respect to r from $r_\mathrm{e} = 0$ to $r_\mathrm{e} = 1$, using the same discretization as for the computation of the mean moisture–precipitation relationships with bin lengths $\Delta r = 0.01$. The results are shown in the third and bottom rows of Figure 5 by the solid black lines. Gray shading in the third row marks the r ranges that contribute to precipitation enhancement over land. The red dashed line in the bottom row indicates the location of maximum increase of the LHS of Equation (6) and, thus, the r value that contributes most to precipitation enhancement over tropical land. We see in all months that precipitation enhancement can be attributed to relatively large humidity values, above $r = 0.6$. The pattern of r ranges identified as contributors can be classified into two types, depending on the considered month. First, a single broad range of values above some threshold value of r. This type is representative for the months from March to July and is the result of the combined effect of the "bump" (if present) and the pronounced tail of the land humidity distribution. The threshold value of r for precipitation enhancement is located between 0.60 and 0.65 in months that exhibit a "bump" and shifted to slightly higher values between 0.65 and 0.70 in months that do not. The second type is representative for the months from August to February and is characterized by an interruption of the broad r range seen in the first type by a range in which precipitation is favored over ocean rather than land. Still, as a whole, precipitation remains favored over land as the LHS of Equation (6) does not become negative. The width of this interruption varies between months and is largest in November, where the ocean has the pronounced high-r tail in its humidity distribution. Such a pronounced tail over ocean is, however, not a necessary condition for causing this interruption.

5 | SENSITIVITY OF THE RESULTS TO THE CHOSEN FIT MODEL

The results presented so far were obtained using empirical fits of the moisture–precipitation relationships over narrow ranges of r, meaning that the shape of the relationships was captured very accurately. Previous studies on $P(r)$, however, have used simple exponential fit models to describe the nature of the relationship (Bretherton *et al.*, 2004; Rushley *et al.*, 2018). Looking at the fairly linear curves of $P(r)$ in log-space as displayed in Figure 2, such an exponential ansatz seems appropriate. In this section, we test whether an exponential ansatz is accurate enough to reconstruct $\chi_\mathrm{bm}(t)$.

There are two ways to obtain a least-squares fit function of the form $P_\mathrm{fit}(r) = a\exp(br)$, analogous to Bretherton *et al.* (2004): either by fitting $P_\mathrm{fit}(r)$ directly to the data, or by transforming $P_\mathrm{fit}(r)$ into the linear function $P_\mathrm{fit,lin}(r) = br + \ln(a)$ and then fitting $P_\mathrm{fit,lin}(r)$ to the data in log-space. The former method minimizes the absolute error of the fit, whereas the latter method minimizes the relative error. We use both methods to compute reconstructions of $\chi_\mathrm{bm}(t)$, accounting for distinct relationships over land and ocean and for the different months, analogous to what was done for Figure 3g with the empirical fit. The results are shown in Figure 6a,b. We find that the exponential ansatz is not able to capture basic characteristics of $\chi_\mathrm{bm}(t)$ regardless of the method chosen (compare with Figure 3g as well).

In Figure 6a, where the fit was obtained with $P_\mathrm{fit,lin}(r)$, both shape and magnitude of the seasonal cycle seem to be captured to some extent, but $\chi_\mathrm{bm}(t)$ is overestimated or underestimated in all months. Looking at the monthly mean values of the precipitation ratio's constituents, $\overline{P_\ell}$ and $\overline{P_\mathrm{o}}$, in Figure 6c, it becomes clear that the similarity between reconstruction and benchmark is spurious since both land and ocean precipitation rates are greatly overestimated throughout the year. This is because the optimization of the relative error leads to large absolute errors, especially for high values of r where precipitation rates are high. When the reconstruction is based on $P_\mathrm{fit}(r)$, as shown in Figure 6b,d, neither shape nor magnitude of $\chi_\mathrm{bm}(t)$ are captured by the reconstruction. In this case, land and ocean mean precipitation are both greatly underestimated. This is because the fit function optimizes for accuracy in the steep, high-r range of $P(r)$ at the expense of accuracy at intermediate r values. At intermediate r values, the fit function remains close to zero whereas the (P, r) bin-mean data already picks up. Thus, we conclude that the deviations of the $P(r)$ mean curves in Figure 2 from a simple analytical form such as an exponential function are significant if the goal is to reconstruct the land–ocean precipitation differences.

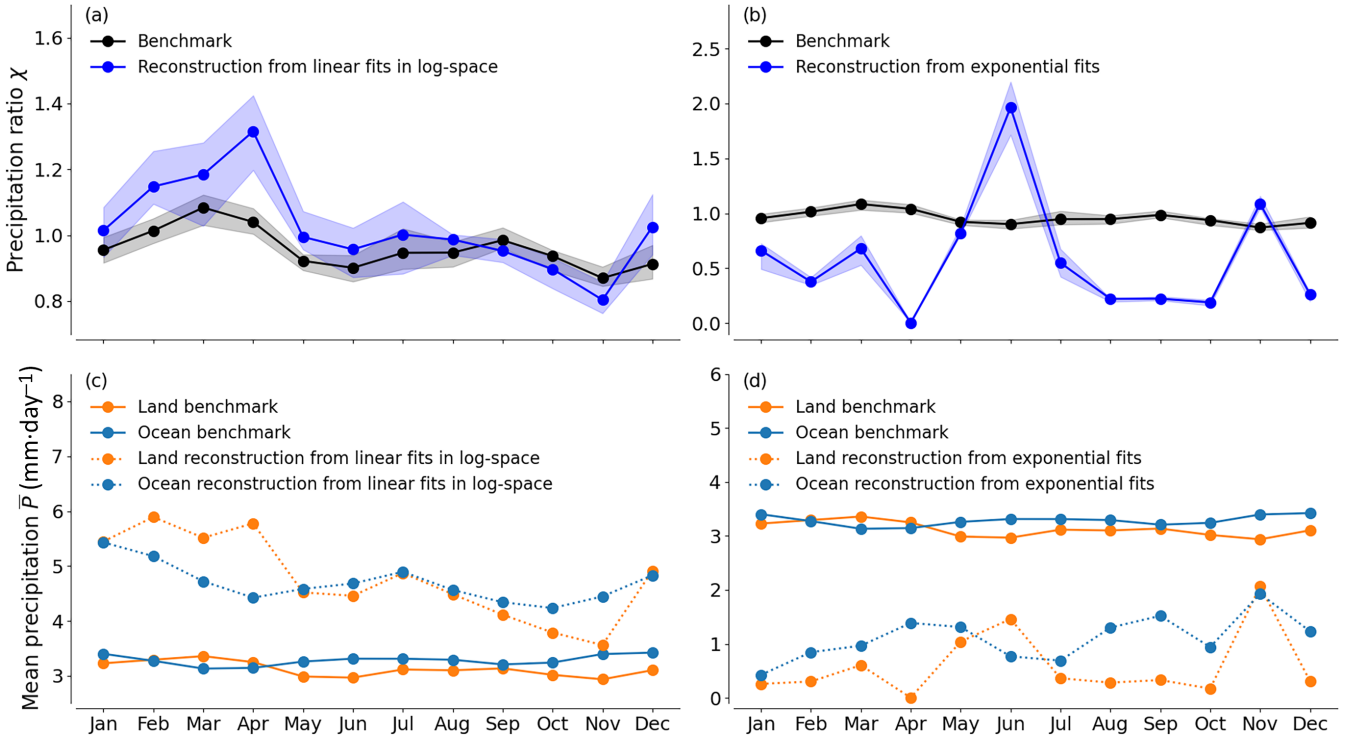

FIGURE 6 Comparison of benchmark values of (a, b) the precipitation ratio and (c, d) the monthly mean precipitation over land and ocean with respective reconstructions based on different analytical fit models. Reconstructions in (a) and (c) are computed using the linear fit model $P_{\mathrm{fit,lin}}(r)$ applied to data in log-space, and reconstructions in (b) and (d) are based on the exponential fit model $P_{\mathrm{fit}}(r)$ applied to data directly. [Colour figure can be viewed at wileyonlinelibrary.com]

That the exponential ansatz is unable to capture the correct value and behavior of a basic mean characteristic of tropical precipitation such as χ raises questions about the usefulness of the concept of a simple, analytical moisture–precipitation relationship in, for instance, the context of conceptual models. In particular, when spatial differences in precipitation characteristics are of interest, a simple form of $P(r)$ will yield spurious results.

6 | SUMMARY AND DISCUSSION

This study investigated whether the moisture–precipitation relationship $P(r)$ is able to explain land–ocean differences in tropical precipitation, quantified by the tropical precipitation ratio χ, and whether the modification of $P(r)$ and/or the modification of the underlying humidity distribution by the land surface enhances land precipitation, as revealed by values of $\chi > 0.86$.

To this end, we first derived the moisture–precipitation relationship from 10 years of daily ERA5 data (1981–1990) and tested to which detail we need to know the spatial and temporal dependence of $P(r)$ in order to adequately reconstruct the mean seasonal cycle and year-to-year variability of $\chi(t)$. Two modes of the variability of $P(r)$ proved to be essential:

1. $P(r)$ is distinct over land and ocean.
2. $P(r)$ exhibits a seasonal cycle.

Using the relationships obtained, $P_{\ell,m}(r)$ and $P_{\mathrm{o},m}(r)$, dependent on surface type (land/ocean) and month, we then showed that, despite the existence of a small range of r values in which $P_{\ell,m}(r)$ lies above $P_{\mathrm{o},m}(r)$ in the months from September to May, the net effect of distinct $P(r)$ relationships over land and ocean in all months is to counteract precipitation enhancement over land. Instead, the precipitation enhancement can be attributed to the influence of land on the humidity distribution.

Over land, the humidity distribution exhibits a more pronounced tail towards high r values. The abundance of these high r values, associated with high rain rates, overcompensates the fact that differences between $P_{\ell,m}(r)$ and $P_{\mathrm{o},m}(r)$ act to reduce precipitation over land compared with over ocean. An exception to this rule is November, where precipitation enhancement requires the additional "support" of the range where $P_{\ell,m}(r) > P_{\mathrm{o},m}(r)$.

Although a correct reconstruction of $\chi(t)$ from the moisture–precipitation relationship proved to be insensitive to the temporal resolution of the underlying data, being averaged either daily or monthly, it does rest on a sufficiently accurate fit $P(r)$. An exponential fit model, as suggested by Bretherton *et al.* (2004) for example, was unable to reproduce basic characteristics of $\chi(t)$ and to explain tropical land–ocean precipitation differences. This insight calls for caution when employing the moisture–precipitation relationship in simple models, especially when spatial variations of precipitation characteristics are of interest.

Since all the results obtained are based on ERA5 data, it must be noted that ERA5 has a number of known biases that may affect the generality of our conclusions. Unfortunately, mismatches between the temporal resolution and/or spatial coverage of data used in existing studies on ERA5 biases and this study make a rigorous assessment of the impact of such biases on our results impossible. Nevertheless, the major sources of uncertainty for our study, arising from precipitation and humidity biases, are worth mentioning.

Compared with observations, ERA5 underestimates the frequency of very low precipitation rates between 0 and 0.25 mm·day^{-1} over tropical oceans, whereas this bias is not found over tropical land (Hassler & Lauer, 2021). Since such low precipitation rates are typically associated with dry environments, this suggests that ERA5 produces too much precipitation at low r values, thereby creating the distinct low-r regime in Figure 2. If the low-r regime were not to exist, and if the moisture–precipitation relationships over land and ocean are otherwise correct, then the role of land–ocean differences in $P(r)$ in causing precipitation enhancement over land may be strengthened.

Regarding humidity biases, ERA5 shows too small values of integrated water vapor over tropical oceans before 1993 (Allan *et al.*, 2022), which could result in too small oceanic r values, provided that ERA5 has fairly realistic vertical profiles of temperature and pressure. However, Wolding *et al.* (2022) report a cold bias in the tropical marine boundary layer that could cause too large oceanic r values, thereby potentially compensating the aforementioned moisture bias at least to some extent.

Though the biases discussed warrant further investigations of the precipitation enhancement over tropical land using independent datasets, such as pure observations or output from convection-resolving model simulations, this study demonstrates that the moisture–precipitation relationship, if constructed with sufficient attention to detail, is a useful tool to probe interactions between tropical precipitation and the underlying surface. It further shows that precipitation enhancement over tropical land is primarily a consequence of how the land modulates column relative humidity, both through direct moistening and heating of the atmospheric column, and through synoptic- or large-scale moisture transport.

ACKNOWLEDGEMENTS

We would like to thank Bjorn Stevens for useful discussions, and Romain Fiévet, as well as three anonymous reviewers for their insightful comments on the manuscript.

DATA AVAILABILITY STATEMENT

The ERA5 data used in this study are made publicly available by the C3S Climate Data Store (https://cds.climate.copernicus.eu).

ORCID

Luca Schmidt https://orcid.org/0000-0003-4319-7571
Cathy Hohenegger https://orcid.org/0000-0002-7478-6275

REFERENCES

Ahmed, F. & Schumacher, C. (2017) Geographical differences in the tropical precipitation-moisture relationship and rain intensity onset. *Geophysical Research Letters*, 44, 1114–1122.

Allan, R.P., Willett, K.M., John, V.O. & Trent, T. (2022) Global changes in water vapor 1979-2020. *Journal of Geophysical Research: Atmospheres*, 127, e2022JD036728.

Austin, J.M. (1948) A note on cumulus growth in a nonsaturated environment. *Journal of the Atmospheric Sciences*, 5, 103–107.

Bretherton, C.S., Peters, M.E. & Back, L.E. (2004) Relationships between water vapor path and precipitation over the tropical oceans. *Journal of Climate*, 17, 1517–1528.

Derbyshire, S.H., Beau, I., Bechtold, P., Grandpeix, J.-Y., Piriou, J.-M., Redelsperger, J.-L. et al. (2004) Sensitivity of moist convection to environmental humidity. *Quarterly Journal of the Royal Meteorological Society*, 130, 3055–3079.

Hassler, B. & Lauer, A. (2021) Comparison of reanalysis and observational precipitation datasets including ERA5 and WFDE5. *Atmosphere*, 12, 1462.

Hersbach, H., Bell, B., Berrisford, P., Biavati, G., Horányi, A., Muñoz Sabater, J. et al. (2018a) *ERA5 hourly data on single levels from 1979 to present*. Copernicus Climate Change Service (C3S) Climate Data Store (CDS). DKRZ.

Hersbach, H., Bell, B., Berrisford, P., Biavati, G., Horányi, A., Muñoz Sabater, J. et al. (2018b) *ERA5 hourly data on pressure levels from 1979 to present*. Copernicus Climate Change Service (C3S) Climate Data Store (CDS). DKRZ.

Hersbach, H., Bell, B., Berrisford, P., Hirahara, S., Horányi, A., Muñoz-Sabater, J. et al. (2020) The ERA5 global reanalysis. *Quarterly Journal of the Royal Meteorological Society*, 146, 1999–2049.

Hohenegger, C. & Stevens, B. (2022) Tropical continents rainier than expected from geometrical constraints. *AGU Advances*, 3, e2021AV000636.

Holloway, C.E. & Neelin, J.D. (2009) Moisture vertical structure, column water vapor, and tropical deep convection. *Journal of the Atmospheric Sciences*, 66, 1665–1683.

Muller, C.J., Back, L.E., O'Gorman, P.A. & Emanuel, K.A. (2009) A model for the relationship between tropical precipitation and column water vapor. *Geophysical Research Letters*, 36, L16804.

Murphy, D.M. & Koop, T. (2005) Review of the vapour pressures of ice and supercooled water for atmospheric applications. *Quarterly Journal of the Royal Meteorological Society*, 131, 1539–1565.

Peters, O. & Neelin, J.D. (2006) Critical phenomena in atmospheric precipitation. *Nature Physics*, 2, 393–396.

Raymond, D.J. & Torres, D.J. (1998) Fundamental moist modes of the equatorial troposphere. *Journal of the Atmospheric Sciences*, 55, 1771–1790.

Rushley, S.S., Kim, D., Bretherton, C.S. & Ahn, M.-S. (2018) Reexamining the nonlinear moisture-precipitation relationship over the tropical oceans. *Geophysical Research Letters*, 45, 1133–1140.

Schiro, K.A., Neelin, J.D., Adams, D.K. & Lintner, B.R. (2016) Deep convection and column water vapor over tropical land versus tropical ocean: a comparison between the amazon and the tropical western pacific. *Journal of the Atmospheric Sciences*, 73, 4043–4063.

Schmidt, L. & Hohenegger, C. (2023) Constraints on the ratio between tropical land and ocean precipitation derived from a conceptual water balance model. *Journal of Hydrometeorology*, 24, 1103–1117.

Tompkins, A.M. (2001) Organization of tropical convection in low vertical wind shears: the role of water vapor. *Journal of the Atmospheric Sciences*, 58, 529–545.

Wolding, B., Powell, S.W., Ahmed, F., Dias, J., Gehne, M., Kiladis, G. et al. (2022) Tropical thermodynamic-convection coupling in observations and reanalyses. *Journal of the Atmospheric Sciences*, 79, 1781–1803.

How to cite this article: Schmidt, L. & Hohenegger, C. (2024) Precipitation enhancement over tropical land through the lens of the moisture–precipitation relationship. *Quarterly Journal of the Royal Meteorological Society*, 1–13. Available from: https://doi.org/10.1002/qj.4838